ANALYSIS OF HIGHER ORDER MULTIPOLES OF THE 952.6 MHz RF-DIPOLE CRABBING CAVIY FOR THE JEFFERSON LAB ELECTRON-ION COLLIDER*

S. U. De Silva[1,2#], S. I. Sosa[1,2], H. Park[2,1], V. S. Morozov[2], J. R. Delayen[1,2]
[1]Center for Accelerator Science, Old Dominion University, Norfolk, VA, USA
[2]Thomas Jefferson National Accelerator Facility, Newport News, VA, USA

Abstract

The crabbing system is a key feature in the Jefferson Lab Electron-Ion Collider (JLEIC) required to increase the luminosity of the colliding bunches. A local crabbing system will be installed with superconducting rf-dipole crabbing cavities operating at 952.6 MHz. The field non-uniformity across the beam aperture in the crabbing cavities produces higher order multipole components, similar to that which are present in magnets. Knowledge of higher order mode multipole field effects is important for accurate beam dynamics study for the crabbing system. In this paper, we quantify the multipole components and analyse their effects on the beam dynamics.

INTRODUCTION

The proposed JLEIC consists of the two figure-8 rings; one for electrons and the other for protons [1]. The electrons are accelerated using the existing CEBAF machine and the ions are accelerated in the linac booster ring as shown in Fig. 1. The luminosity goal of the JLEIC is in the range of 10^{33} to 10^{34} cm^{-2}sec^{-1} per interaction point.
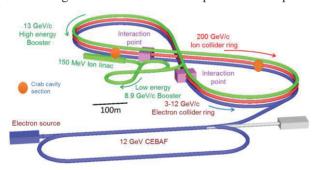

Figure 1: JLEIC electron and ion collider rings.

The high luminosity operation of the JLEIC requires the electron and proton bunches to collide head-on, hence increasing the number of interactions between the colliding bunches [2]. A local crabbing system will be developed with rf-dipole crabbing cavities operating at 952.6 MHz. Two crabbing sections will be installed before and after each interaction point (IP) on both electron and proton rings, in order to crab and to cancel the crabbing effect on the beam.

JLEIC is designed to operate at several center of mass (CM) energies with different beam currents [1]. Therefore,

the total crabbing kick required at different energies depend on corresponding beam energy and beam parameters with maximum electron and proton beam energies of 12 GeV and 200 GeV, respectively. The total crabbing kick is determined by Eq. (1) with beam parameters given in Table 1 [3].

$$V_t = \frac{cE_b \tan\left(\frac{\varphi_{crab}}{2}\right)}{2\pi f_{rf} \sqrt{\beta_x^* \beta_x^c}} \quad (1)$$

where E_b is the beam energy, φ_{crab} is the crossing angle, β_x^* is the betatron function at IP, β_c^* is the betatron function at the location of the crabbing cavity. Table 1 lists the total crabbing kick for the two highest energies for both electron and proton beams. The increase in β_x^* for 200 GeV proton beam energy allows to maintain the total crabbing kick voltage with only a 24% increase.

Table 1: JLEIC Crab Crossing Design Parameters

Parameter	Electron		Proton		Units
E_b	10	12	100	200	GeV
f_{rf}	952.6				MHz
φ_{crab}	50				mrad
β_x^*	9.1	6.6	8	2.1	cm
β_c^*	200	200	650	650	m
V_t	3.0	4.2	17.4	21.5	MV

JLEIC CRABBING CAVITY DESIGN

The crabbing cavity design for JLEIC requires a cavity operating at 952.6 MHz with a beam aperture of 70 mm. The high operating frequency and large beam aperture make it challenging in designing a cavity with low peak surface field ratios and high shunt impedance, which are the key properties for any superconducting rf cavity.

Several crabbing cavity geometries have been studied including squashed elliptical cavity, rf-dipole cavity with single cell, 2 cells, and 3 cells [4]. The 2-cell rf-dipole shown in Fig.2 has been selected as the JLEIC crabbing cavity design. The electromagnetic field on the 2-cell rf-dipole cavity is shown in Fig. 3. The design details and rf properties are presented in Table 2. The maximum peak magnetic field for the crabbing cavities is decided to be 70 mT in order to operate at moderate surface fields. Therefore, the maximum transvers voltage achievable by the 2-cell rf-dipole cavity is limited to be 1.9 MV. Table 3 lists the number of cavities required per side per beam for

both electron beam and proton beams and the peak fields at which the cavities would operate.
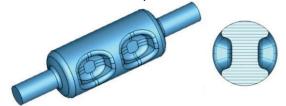

Figure 2: 952.6 MHz 2-cell rf-dipole crabbing cavity with cross section.
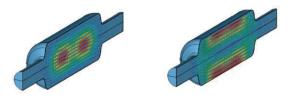

Figure 3: Electric (left) and magnetic (right) fields in the 952.6 MHz 2-cell rf-dipole crabbing cavity.

Table 2: RF properties of 952.6 MHz 2-cell rf-dipole crabbing cavity

Parameter	Value	Units
SOM	849.7	MHz
Nearest HOM	1395.4	MHz
Peak electric field (E_p*)	5.8	MV/m
Peak magnetic field (B_p*)	11.7	mT/(MV/m)
Geometrical factor (G)	171.4	Ω
$[R/Q]_t$	150.5	Ω
$R_t R_s$	$2.6 \times 10^\$$	Ω^2

* At E_t^* = 1 MV/m

Table 3: Crabbing Cavity Properties for Electron and Proton Beams

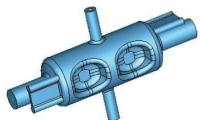| Parameter	e	p	Units
E_b	12	200	GeV
V_t per cavity	1.4	1.9	MV
E_p	26	35	MV/m
B_p	53	71	mT
No. of cavities per beam per side	3	12	

Figure 4: 952.6 MHz 2-cell rf-dipole crabbing cavity with HOM couplers.

The detailed higher order mode (HOM) damping scheme for the JLEIC crabbing cavities is being developed [4]. The preliminary HOM coupler design for the 2-cell cavity is shown in Fig. 4.

MULTIPOLES IN A RF CAVITY

In deflecting/crabbing cavities the time dependent rf field of the fundamental operating mode varies across the beam aperture leading to field non-uniformity. This field variation can be quantified in terms of higher order multipole components similar to magnets [5, 6].

Multipole field components $E_{acc}^{(n)}$ with order n can be determined by Fourier series expansion of the electromagnetic fields in the cavity given by

$$E_{acc}^{(n)}(z) = \frac{1}{r^n} \int_0^{2\pi} E_z(r,\phi,z) e^{in\phi} e^{i\omega t} d\phi \quad (1)$$

where $E_z(r,\phi,z) = \sum_{n=0}^{\infty} E_z^{(n)}(z) r^n e^{in\phi}$ is the on-axis electric field in the cavity. The higher order multipole components can be calculated using Panofsky Wenzel theorem [7] as

$$A^{(n)} + iB^{(n)} = \frac{1}{qc} F_t^{(n)}(z) = i\frac{n}{\omega} E_{acc}^{(n)}(z), \quad (2)$$

$$a_n + ib_n = \int_{-\infty}^{\infty} \left(A^{(n)}(z) + B^{(n)}(z) \right) dz. \quad (3)$$

where a_n and b_n are skew and normal multipole components. The skew components are zero for the rf-dipole cavity. The b_1 component corresponds to the transverse voltage and b_0 component corresponds to the accelerating voltage in the cavity.

MULTIPOLE FIELD ANALYSIS

The electromagnetic fields are extracted using very high meshed cavity model simulated in CST Microwave Studio [8]. The higher order multipole components are calculated using the method described above for the 952.6 MHz 2-cell rf-dipole cavity shown in Fig. 2. The multipole components normalized to a transverse voltage of 1 MV are listed in Table 4.

Table 4: Higher Order Multipole Components for the Bare Cavity and Cavity with HOM Couplers

Component	Bare Cavity	Cavity with HOMs	Units
V_{acc}	2.5×10^{-4}	12.7	kV
V_t	1.0	1.0	MV
b_1	3.33	3.33	mT m
b_2	-1.9×10^{-4}	0.85	mT
b_3	968.5	971.7	mT/m
b_4	0.4	103.5	mT/m^2
b_5	-4.1×10^4	-4.1×10^4	mT/m^3
b_6	-641.5	1702.8	mT/m^4
$_7$	-7.0×10^7	-7.2×10^7	mT/m^5
Δx	1.3	634.1	μm

The cavity geometries with symmetry contributes only to odd components (b_1, b_3, b_5…) while the even components (b_2, b_4, b_6…) are zero. The b_0 component is zero by definition given in Eq. (2), however the integrated component corresponds to an on-axis accelerating voltage (V_{acc}) present in the cavity. The rf-dipole cavity with symmetry has zero E_z component on axis with negligible V_{acc} component. A higher on-axis V_{acc} component results in a shift in the cavity electrical center with respect to the mechanical center. This requires the cavities to be aligned with the beam at the electrical center to avoid beam coupling with the V_{acc} component.

Similarly, the higher order multipole components are calculated for the 2-cell rf-dipole cavity with HOM couplers shown in Fig. 4. The multipole components are listed in Table 4. The asymmetry in the cavity geometry due to presence of the HOM couplers increases the contribution from even multipole components, however, doesn't lead to a significant change in the odd components. In addition, the shift in the electrical center for the cavity with HOM couplers is 634.1 μm, which is a significant increase compared to the bare cavity.

BEAM DYNAMICS OF THE MULTIPOLES

The crabbing cavities for both the proton and electron rings are placed in the straight section just before the bends. The crabbing cavities in the proton ring are placed in the chromaticity compensation blocks in order to have higher β_x^* that would reduce the required crabbing cavity voltage [9]. The effects of higher order multipole components are studied in estimating the effect on dynamic aperture (DA). The analysis is carried out in elegant [10] using Multipole RF DeFlector (MRFDF) elements.
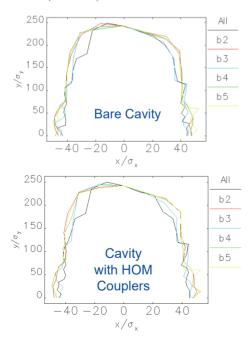

Figure 5: Electric field (left) and magnetic field (right) in the 952.6 MHz 2-cell rf-dipole crabbing cavity.

The DA is investigated with the crabbing cavity higher order multipole components for the proton beam for over 2000 turns and scanned in the x-y plane along 55 rays. The reference DA of ± 50 σ_x due to the linear kick is studied with multipole components b_2-b_5. As shown in Fig. 5 the DA is is reduced to ± 46 σ_x for both bare cavity and the cavity with HOM couplers. The major limitation to the DA of ± 10 σ comes from the final focusing quadrupoles. Therefore, the effects on DA due to crabbing higher order multipole components are negligible.

CONCLUSION

The 952.6 MHz 2-cell rf-dipole crabbing cavity design has been selected for the JLEIC crabbing. The analysis of the complete HOM damping scheme is ongoing. The higher order multipole components have been calculated numerically for the 952.6 MHz 2-cell rf-dipole crabbing cavity. The multipole components are compared between the bare cavity and the cavity with HOM couplers. The presence of crabbing cavities in the ion ring was simulated to study the effects of the multipole components on dynamic aperture. The b_5 component is the limiting component with larger effect on dynamic aperture. However, this effect from the crabbing cavities are insignificant compared to that from final focusing quadrupole magnets.

REFERENCES

[1] Y. Zhang, "JLEIC: A High Luminosity Polarized Electron-Ion Collider at Jefferson Lab", presented at IPAC'19, Melbourne, Australia, 2019, TUPRB112, this conference.

[2] R. B. Palmer, "Energy scaling, crab crossing and the pair problem", SLAC-PUB-4707, 1988.

[3] Y.-P. Sun *et.al.*, *Phys. Rev. Accel. Beams* **12**, 101002, 2009.

[4] H. Park, S.U. De Silva, S. I. Sosa, J.R. Delayen, "Design of a Proof-of-principle Crabbing Cavity for the Jefferson Lab Electron-Ion Collider", presented at IPAC'19, Melbourne, Australia , 2019, WEPRB093, this conference.

[5] J. Barranco Garcia *et.al.*, *Phys. Rev. Accel. Beams* **19**, 101003, 2016.

[6] S.U. De Silva, H. Park, J.R. Delayen, in *Proc. IPAC'17*, Copenhagen, Denmark, 2017, p. 1177.

[7] W.K.H. Panofsky and W.A. Wenzel, *Rev. Sci. Instrum.* **27**, 967, 1956.

[8] CST Microwave Studio, https://www.cst.com.

[9] S.I. Sosa, S.U. De Silva, J.R. Delayen, V.S. Morozov, in *Proc. IPAC'17*, Copenhagen, Denmark, 2017, p. 3025.

[10] M. Borland, "elegant: A Flexible SDDS-Compliant Code for Accelerator Simulation", *Advance Photon Source* LS-28, September 2000.